Polymer Journal, Vol. 3, No. 4, pp 488—499 (1972)

Light Scattering Patterns from Crystalline Textures in Nonspherical Symmetry*

Susumu TATEMATSU,** Norio HAYASHI, Shunji NOMURA, and Hiromichi KAWAI†

Department of Polymer Chemistry, Faculty of Engineering, Kyoto University, Kyoto, Japan.

(Received October 23, 1971)

ABSTRUCT: The polarized light scattering from the crysalline texture in nonspherical symmetry was discussed with a two dimensional approximation. The calculations were performed in terms of the series expansion of the shape factor in the fundamental equation of amplitude of scattered ray in order to formulate the scattering intensity distribution from the asymmetric bodies in general.

The polarized scattering intensity distributions, $I(\theta, \mu)_{H_V}$ and $I(\theta, \mu)_{V_V}$, were discussed for the following three types of crystalline textures in nonspherical symmetry; sheaf-like, N-regular polygonal, and eccentric circular textures. It was concluded that the intensity distributions change considerable having finite intensities at $\mu=0°$ and 90° for the $I(\theta, \mu)_{H_V}$, and that the intensity, $I(0, \mu)_{H_V}$, does not necessarily become zero, both events occurring when the texture deviates from the circular disc.

KEY WORDS Light Scattering / Crystalline Texture / Shape Factor / Scattering Intensity /

The polarized light scattering from spherulitic films of crystalline polymers was studied first by Stein and his coworkers[1,2] on the basis of an idealized spherulitic crystalline texture. They assumed that the optical anisotropy of the spherulite in spherical symmetry is given by $(\alpha_r-\alpha_t)$ irrespective of the position within the spherulite, where α_r and α_t are polarizabilities along the radial and tangential directions of the sherulites dispersed in a uniform medium of polarizability α_s, and that there is neither a size distribution nor an optical correlation among the dispersed spherulites. In other words, the scattering from an isolated single spherulite of idealized regular texture has been proposed.

Although the polarized light-scattering pattern from well-grown spherulites, such as the pattern from annealed linear polyethylene film, follows the above perfect spherulitic scattering, most of the scattering patterns from law and medium density polyethylene films do not necessarily follow the perfect spherulitic scattering,[3] probably because of considerable differences in crystalline texture from the idealized spherulitic one.

In the previous paper in this series,[3] the deviations of the polarized light-scattering patterns from low- and medium-density polyethylene films were discussed by taking the distribution of size of the spherulite into account, taking the spherulite anisotropy, $(\alpha_r-\alpha_t)$, as a function of distance from the center of the spherulite, making the boundary of the spherulite less clear, and changing the crystalline texture from the spherulitic to the sheaf-like. The former two modifications did not significantly change the intensity distribution of the polarized light scattering from that due to perfect spherulitic scattering, except for some shift of the scattering angle at maximum intensity. The latter two modifications have reproduced, at least qualitatively, the actual spherulitic scattering, suggesting that the imperfection of

* Presented at the 20th Annual Meeting of the Society of Polymer Science, Japan, Tokyo, May 27, 1971.

** Present address: *Central Research Laboratory, Dai-Nippon Ink and Chemicals Inc., 2-7-8, Kamikizaki, Urawa, Saitama, Japan.*

† To whom all correspondence should be addressed.

the spherulitic texture, not only in the sense of the texture itself but also in the regularity of its anisotropy, plays an important role.

The modification of the idealized crystalline texture in spherical symmetry to asymmetric types, such as truncated spherulitic and polygonal as well as sheaf-like, have been discussed by Picot, *et al.*[4,5] on the basis of two-dimensional approximation. The other modifications of making the spherulite anisotropy less regular have been performed by Stein and his coworkers[6-8] using mainly the statistical approach involving the theory of random correlation of fluctuation of either orientation or optical anisotropy of the scattering elements within the spherulite.

In this paper, the former modifications of the crystalline texture in spherical symmetry to asymmetrical types, will be further discussed also on the basis of a two dimensional approximation but a more general treatment for the asymmetry (including not only the sheaf-like and regular polygonal textures but also eccentric circular textures) will be used.

CALCULATIONS

The calculations will be worked out for the case of two-dimensional system because of the mathematical simplicity and the limited computer time for numerical calculations. The three-dimensional system must be, in reality, the more common crystalline texture to which the theory should be extended. The theory for the two-dimensional system, *i.e.*, the two-dimensional approximation, however, is believed to show fundamental features of light scattering which are, at least qualitatively, common to the two- and three-dimensional systems.[9,10] In fact, the scattering from two- and three-dimensianal spherulites are very similar unless the faces of two-dimensional spherulites are oblique to the incident beam.[11]

The intensity of scattered light from a random assembly of two-dimensional anisotropic bodies may be given by

$$I(\theta, \mu)=K\int_0^{2\pi} E(\theta_j)\cdot E^*(\theta_j)\,\mathrm{d}\theta_j \qquad (1)$$

where θ and μ are the scattering and asimuthal angles of the scattered ray, respectively, both with respect to the optical coordinates of $0\text{-}i_1i_2i_3$, as illustrated in Figure 1. θ_j is the angle between the i_3 axis and the j_3 axis fixed within the two-dimensional anisotropic body, as demonstrated in Figure 2, for defining the rotation of the body and $E(\theta_j)$ is the amplitude of the scattered ray, as given by

$$E(\theta_j)=\int_{\omega=0}^{2\pi}(\boldsymbol{M}\cdot\boldsymbol{o})\int_{r=0}^{R(\omega)}\exp\left[ik(\boldsymbol{r}\cdot\boldsymbol{s})\right]r\,\mathrm{d}r\,\mathrm{d}\omega \qquad (2)$$

where $\boldsymbol{M}$ is the induced dipole moment, $\boldsymbol{o}$ is a unit vector along the polarization direction of

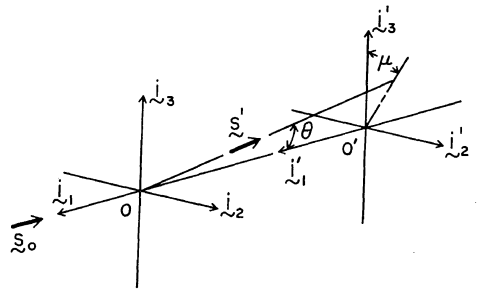

Figure 1. Schematic diagram showing the coordinates system of light scattering.

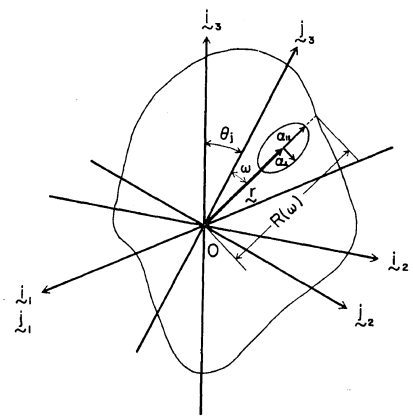

Figure 2. Schematic diagram showing the geometrical relations of a two-dimensional anisorpic body and a scattering element within that body both with respect to the coordinates system of light scattering.

* The two-dimensional system means that the two-dimensional anisotropic bodies orient within the i_2i_3 plane in Figure 1, to which the incident beam, s_0 is radiated along the i_1 axis.

the analyzer, s is the scattering vector defined by (s_0-s'), r is the position vector of the scattering element within the two-dimensional the radius of body, an $R(\omega)$ is the radius of the body as a function of angle ω for characterizing the shape of the body.

Substituting eq 2 into eq 1, the polarized scattering intensities under the H_v and V_v polarization conditions may be given by*

$$I(\theta, \mu)_{H_v}=\frac{K\delta^2E_0^2R_0^4}{4}\{A_1(\theta)-A_2(\theta)\cos 4\mu\} \quad (3)$$

and

$$I(\theta, \mu)_{V_v}=\frac{K\delta^2E_0^2R_0^4}{4}\{A_1(\theta)+A_2(\theta)\cos 4\mu +(1+2p)A_3(\theta)\cos 2\mu+(1+2p)^2A_4(\theta)\} \quad (4)$$

where δ is a parameter defined by $(\alpha_{/\!/}-\alpha_\perp)$ for representing the optical anisotropy of the scattering element, and $p=(\alpha_\perp-\alpha_s)/(\alpha_{/\!/}-\alpha_\perp)$.

As recognized from eq 3, the H_v scattering pattern has four-fold symmetry; *i.e.*,

$$I(\theta, \pm\mu)_{H_v}=I(\theta, \pi/2\pm\mu)_{H_v}=I(\theta, \pi\pm\mu)_{H_v} =I(\theta, 3\pi/2\pm\mu)_{H_v} \quad (5)$$

and the scattering intensities at two particular azimuthal angles, $\mu=0°$ and 45°, can be given by

$$I(\theta, 0)_{H_v}=\frac{K\delta^2E_0^2R_0^4}{4}\{A_1(\theta)-A_2(\theta)\} \quad (6)$$

and

$$I(\theta, \pi/4)_{H_v}=\frac{K\delta^2E_0^2R_0^4}{4}\{A_1(\theta)+A_2(\theta)\} \quad (7)$$

As again recognized from eq 6 and 7, the scattering angle dependences of A_1 and A_2 can be determined from measurable quantities, $I(\theta, 0)_{H_v}$ and $I(\theta, \pi/4)_{H_v}$, and, subsequenntly, the H_v scattering intensity at any given θ and μ can be predicted from the A_1 and A_2 thus determined; *i.e.*,

$$(1/2)\{I(\theta, 0)_{H_v}+I(\theta, \pi/4)_{H_v}\}=\frac{K\delta^2E_0^2R_0^4}{4}A_1(\theta) \quad (8)$$

and

$$(1/2)\{I(\theta, 0)_{H_v}-I(\theta, \pi/4)_{H_v}\}=\frac{-K\delta^2E_0^2R_0^4}{4}A_2(\theta)\,. \quad (9)$$

Similarly from the V_v scattering, the scattering angle dependences of A_3 and A_4 can be determined from measurable quentities, $I(\theta, 0)_{V_v}$, $I(\theta, \pi/2)_{V_v}$, and $I(\theta, \pi/4)_{V_v}$, and, subsequently, the V_v scattering intensity at any given θ and μ can be predicted from the A_1, A_2, A_3, and A_4 thus determined, providing that the parameter p, the polarizability difference between the medium and the scattering element, is known from another source; *i.e.*,

$$I(\theta, \pi/4)_{V_v}-I(\theta, 0)_{H_v}=\frac{K\delta^2E_0^2R_0^4}{4}(1+2p)^2A_4(\theta) \quad (10)$$

and

$$(1/2)\{I(\theta, 0)_{V_v}-I(\theta, \pi/2)_{V_v}\} =\frac{K\delta^2E_0^2R_0^4}{4}(1+2p)A_3(\theta) \quad (11)$$

Figure 3 demonstrates the scattering angle

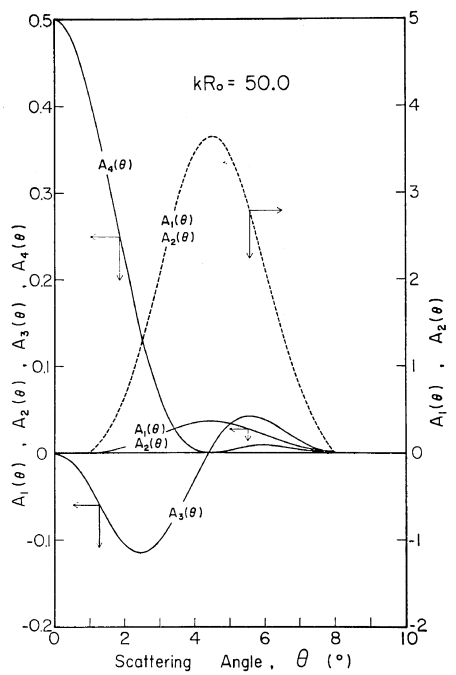

Figure 3. Scattering angle dependences of A_1, A_2, A_3, and A_4 for a random assembly of two-dimensional perfect spherulites (circular discs).

* These derivations will be discussed in detail in the appendix.

dependence of A_1, A_2, A_3, and A_4 for a random assembly of perfact two-dimensional spherulites (circular disc) for which $A_1=A_2$, $A_1(0)=0$, and $I(\theta, 0)_{H_V}$ and $I(0, 0)_{H_V}$ are zero. As will be discussed latter, when the shape of the anisotropic body deviates from that of a circular disc, the value of A_1 differs from that of A_2 and the value of $A_1(0)$ also differs from zero. As seen in the figure, the V_V scattering mostly arises from A_3 and A_4 over a range of scattering angles less than about 4° and from A_3 over a range of scattering angles greater than about 4°.

The modifications of the two-dimensional anisotropic body from circular symmetry to other asymmetric shapes, will be performed through the function $R(\omega)$; *i.e.*, by taking $R(\omega)$ as a sort of step function to obtain the sheaf-like structure, taking $R(\omega)$ as given by

$$R(\omega)=\frac{R_{\max}\cos\omega_0}{\cos\omega} \tag{12}$$

to give an element of regular polygons, and taking $R(\omega)$ as given by

$$R(\omega)=R_0(1+b\cos 2\omega) \tag{13}$$

or

$$R(\omega)=R_0(1+c\cos\omega) \tag{14}$$

to give double or single eccentric circular disc,

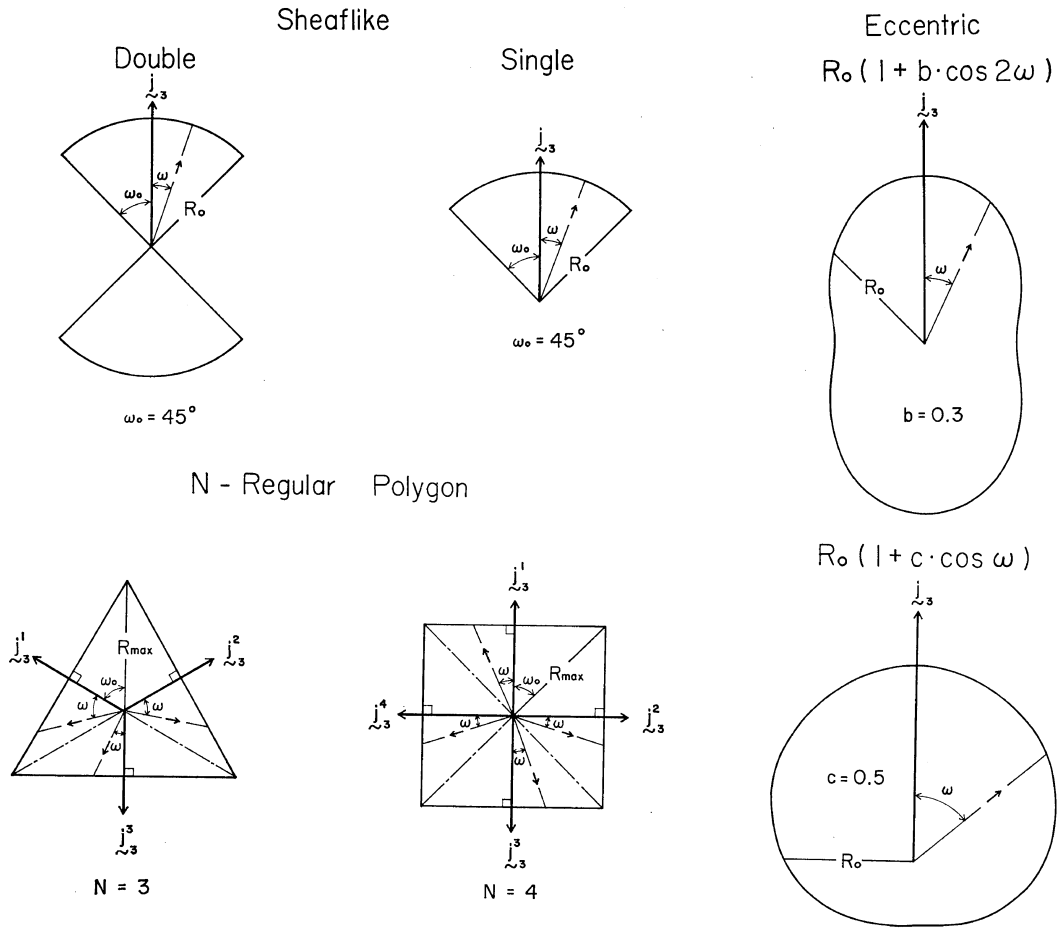

Figure 4. Five types of asymmetric bodies; sheaf-like (double) (Model I), sheaf-like (single) (Model II), *N*-regular polygonal (Model III), eccentric circular disc (double) (Model IV), and eccentric circular disc (single) (Model V) Textures, formulating $R(\omega)$ as step function and as given by eq 12 to 14, respectively, so as to deviate the textures from circular symmetry.

respectively, under the limitation of $0 \leqq b \leqq 1$ or $0 \leqq c \leqq 1$, where $b=0$ or $c=0$ corresponds to the circular disc. Figure 4 illustrates some examples of the respective formulations of $R(\omega)$ for sheaf-like (double) (Model I), sheaf-like (single) (Model II), N-regular polygon (Model III), eccentric circular disc (double) (Model IV), and eccentric circular disc (single) (Model V).

RESULTS AND DISCUSSIONS

Figures 5 to 9 show the calculated results for relative intensity distribution of the H_V scattering at particular azimuthal angles, $\mu=0°$ and 45°, $I_r(\theta, 0)_{H_V}$ and $I_r(\theta, \pi/4)_{H_V}$, for the respective models, Model I through Model V, where the relative intensity distribution is defined by

$$I_r(\theta, \mu)_{H_V}=\frac{I(\theta, \mu)_{H_V}}{K\delta^2 E_0^2 S^2} \tag{15}$$

and S is the surface area of the respective models.

As seen in the figures, the intensity distributions from Model I and Model IV resemble each other, and those from Model III and Model V also resemble each other. Thus, for Model I and Model IV, the intensity distribution along either $\mu=0°$ or 45° has, at least, two maxima including a maximum at $\theta=0°$; whilst for the Model III and Model V, the intensity distribution along $\mu=0°$ has also, at least, two maxima, neither of which appears at $\theta=0°$, and that along $\mu=45°$ has, at least, one maximum not at $\theta=0°$ but at a given scattering angle.

In detail, however, the intensity distribution, especially along $\mu=45°$, differs between the Models I and IV; *i.e.*, for the Model I, whose average radius is given by

$$\bar{R}=(1/2\pi)\int_0^{2\pi} R(\omega)\,\mathrm{d}\omega \tag{16}$$

and is usually much affected by ω_0 to give a considerably smaller value than R_0, the scattering angle at maxmum intensity, θ_{max} ($\neq 0$), is hardly changed with the parameter ω_0. However for the Model IV, whose average radius is always R_0 irrespective of b, the θ_{max} is shifted to smaller scattering angles with increases in the

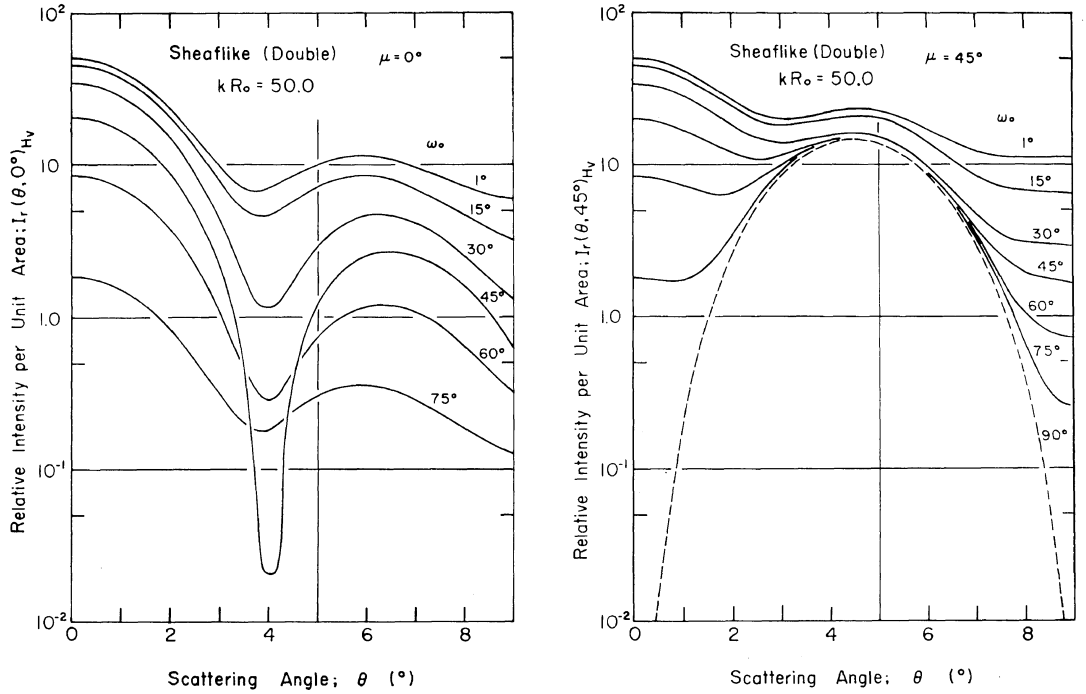

Figure 5. Intensity distributions of scattered rays under the H_V polarization at particular azimuthal angles, $\mu=0°$ and 45°, from the sheaf-like texture (model I) having various values of ω_0.

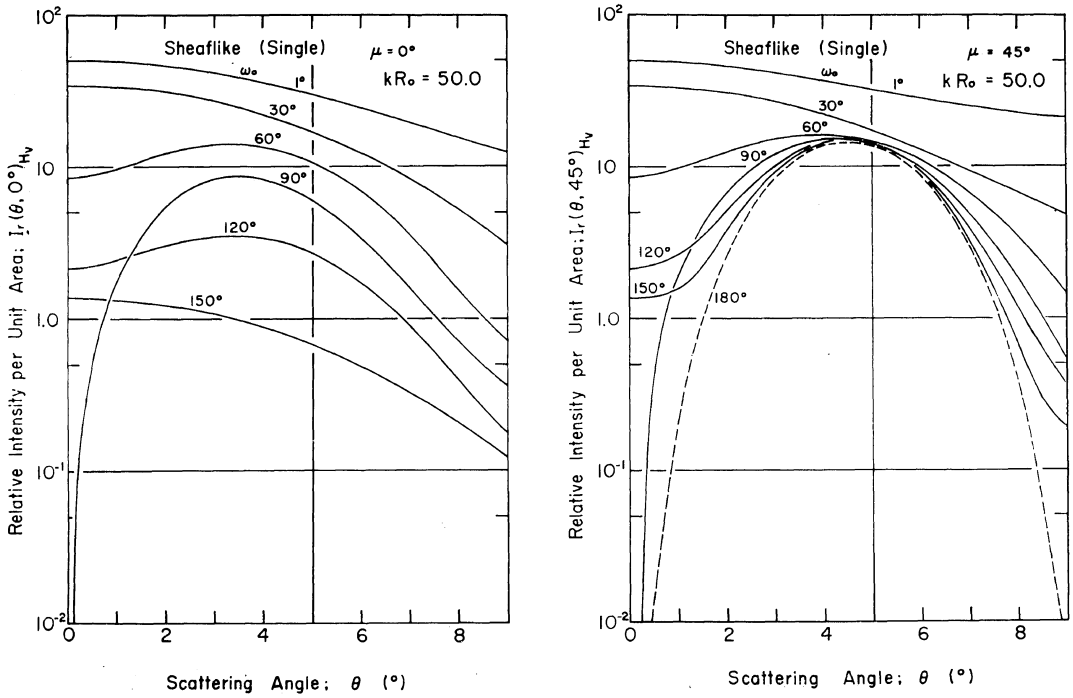

Figure 6. Intensity distributions of scattered rays under the H_V polarization at particular azimuthal angles, μ=0° and 45°, from the sheaf-like texture (Model II) having various values of ω_0.

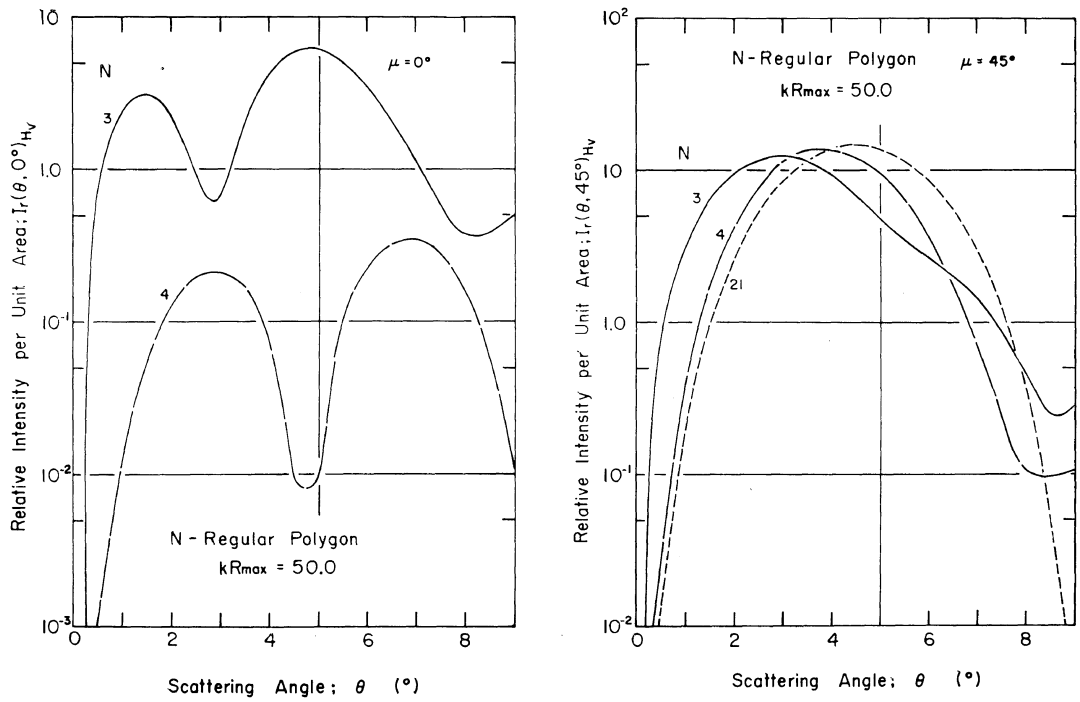

Figure 7. Intensity distributions of scattered rays under the H_V polarization at particular azimuthal angles, μ=0° and 45°, from the N-regular polygonal texture (Model III) having various values of N.

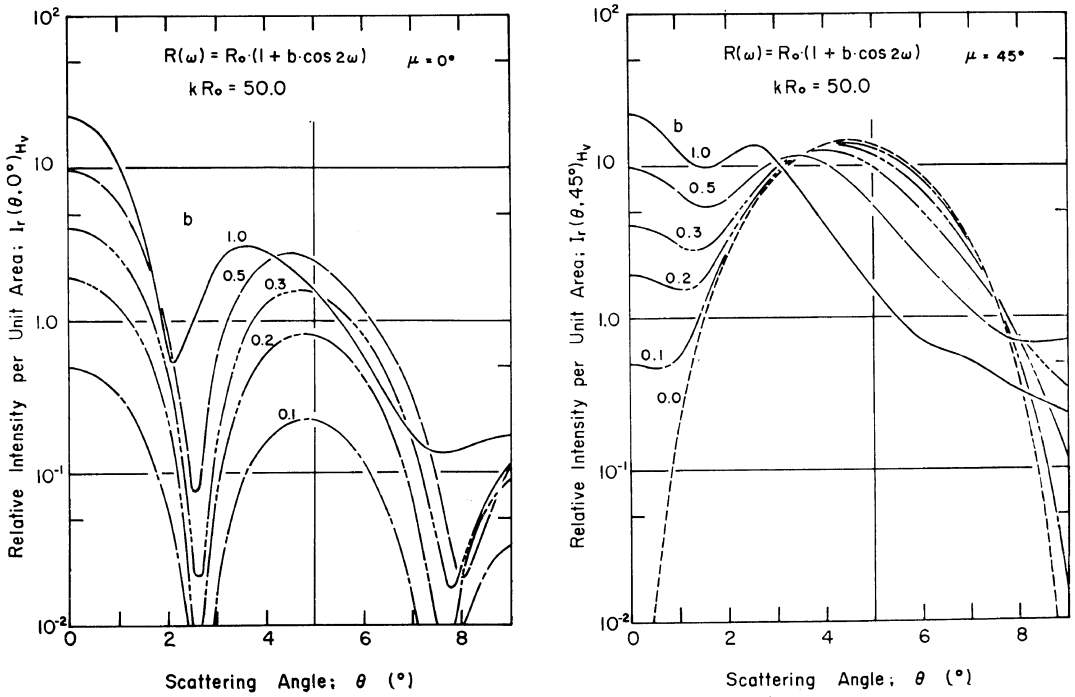

Figure 8. Intensity distributions of scattered rays under the H_V polarization at particular azimuthal angles, μ=0° and 45°, from the eccentric circular disc texture (Model IV) having various values of b.

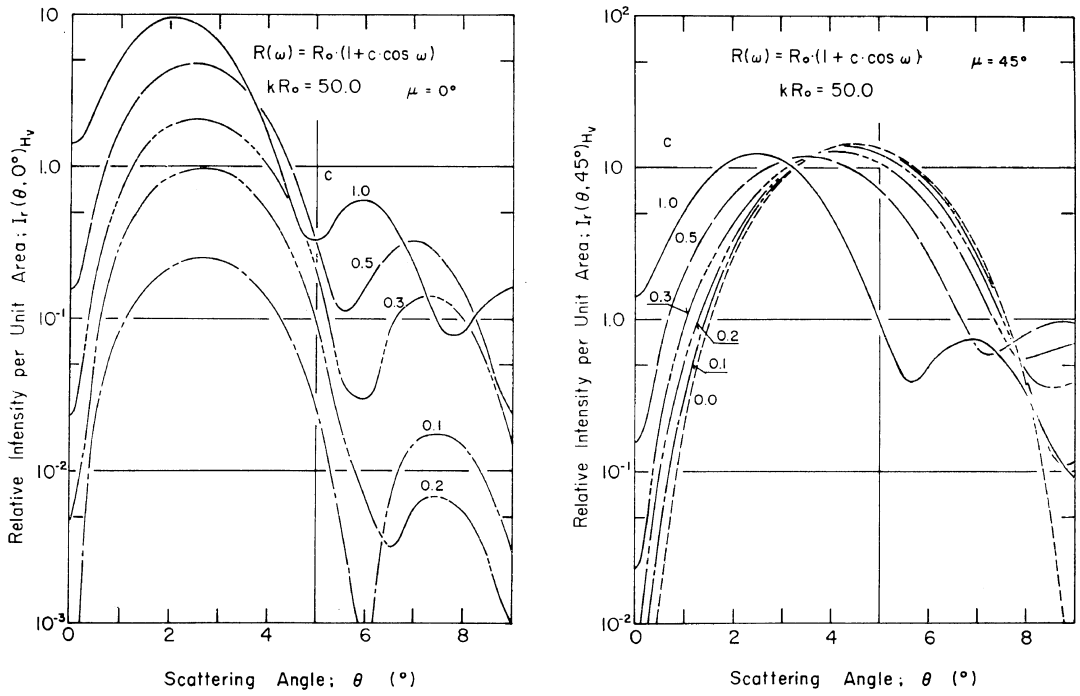

Figure 9. Intensity distributions of scattered rays under the H_V polarization at particular azimuthal angles, μ=0° and 45°, from the eccentric circular disc texture (Model V) having various values of c.

parameter b, suggesting that the contribution to the scattering intensity from the portion of $R(\omega)>R_0$ is much greater than that from the residual portion of $R(\omega)<R_0$. For the Model II, whose average radius is also much affected by ω_0 and is usually considerably smaller than R_0, the θ_{max} is also hardly changed with ω_0, unless ω_0 is smaller than 60°. For the N-regular polygen, Model III, having $N=3, I(0, \mu)_{H_V}$ becomes zero, and that $N=5$, the scattering intensity distribution becomes identical to that of the circular disc.

From eq 1 and 2, $I(0, \mu)_{H_V}$ can be written as

$$I(0, \mu)_{H_V}=K\int_{\theta_j=0}^{2\pi}\left\{(\boldsymbol{M}\cdot\boldsymbol{o})\frac{[R(\omega)]^2}{2}\mathrm{d}\omega\right\}^2\mathrm{d}\theta_j \quad (17)$$

$$=\frac{K\pi\delta^2E_0^2}{16}\left[\int_0^{2\pi}\{R(\omega)\}^2\cos 2\omega\,\mathrm{d}\omega\right]^2 \quad (18)$$

which gives

$$I_r(0, \mu)_{H_V}=\pi\left[\frac{\int_0^{2\pi}\{R(\omega)\}^2\cos 2\omega\,\mathrm{d}\omega}{\int_0^{2\pi}\{R(\omega)\}^2\,\mathrm{d}\omega}\right]^2 \quad (19)$$

For the respective models, eq 19 may be rewritten as follows: for Models I and II

$$I_r(0, \mu)_{H_V}=\pi\frac{\sin^2 2\omega_0}{4\omega_0^2} \quad (20)$$

for Model III

$$I_r(0, \mu)_{H_V}=0 \quad (21)$$

for Model IV

$$I_r(0, \mu)_{H_V}=\pi\frac{4b^2}{4+4b^2+b^4} \quad (22)$$

and for Model V

$$I_r(0, \mu)_{H_V}=\pi\frac{e^4}{4(4+4e^2+e^4)} \quad (23)$$

In addition, for the single-truncated circular disc proposed by Picot[5]

$$I_r(0, \mu)_{H_V}=\pi\left\{\frac{G^2\cos^{-1}G-G(1-G^2)^{1/2}}{\pi-\cos^{-1}G+G(1-G^2)^{1/2}}\right\}^2 \quad (24)$$

where G is defined by $\cos\omega_0$, as illustrated in Figure 12, later.

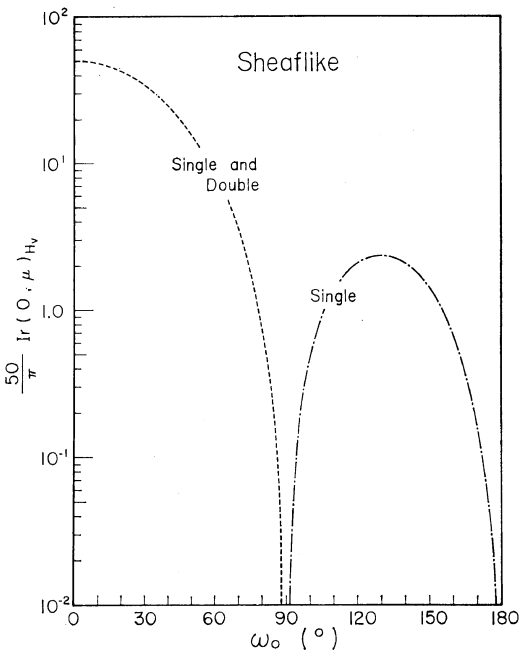

Figure 10. Changes of relative intensity of scattered rays under the H_V polarization, $I_r(0, \mu)_{H_V}$, with the parameter ω_0 for the sheaf-like textures (Model I and Model II).

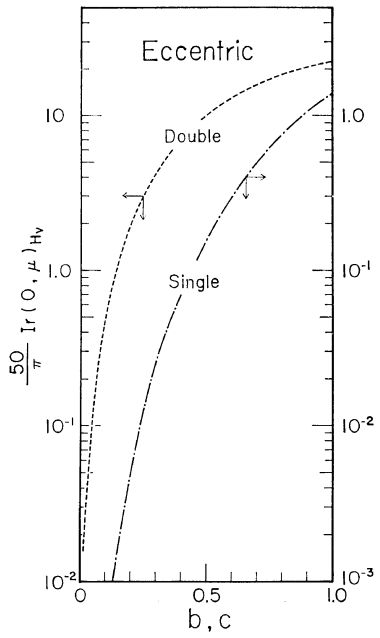

Figure 11. Changes of relative intensity of scattered rays under the H_V polarization, $I_r(0, \mu)_{H_V}$, with the parameters b and c for the eccentric circular disc textures (Model IV and Model V), respectively.

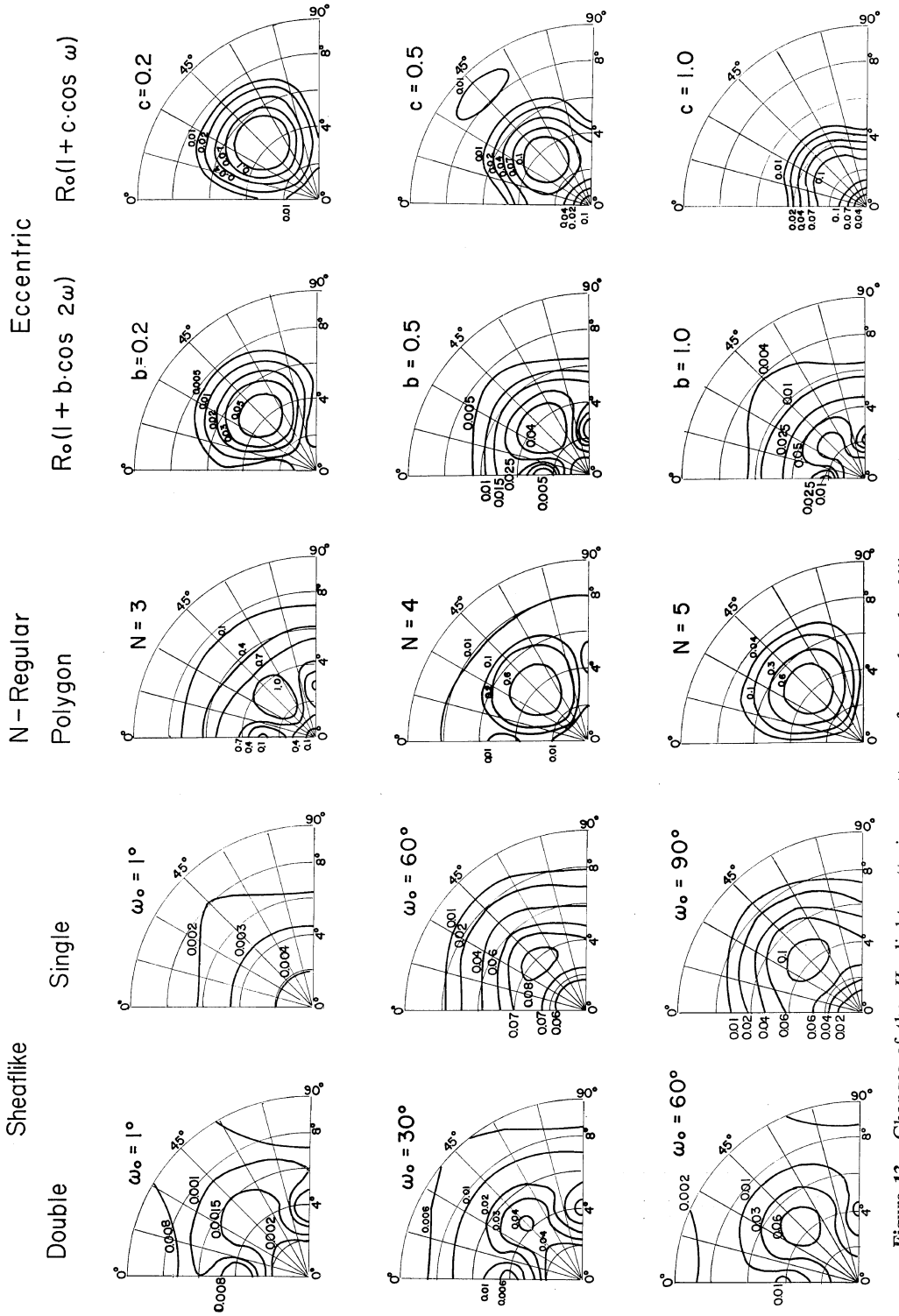

Figure 13. Changes of the H_v light-scattering patterns from the sheaf-like, N-regular polygonal, and eccentric circular disc textures with the parameters, ω_0, N, and a and c, respectively.

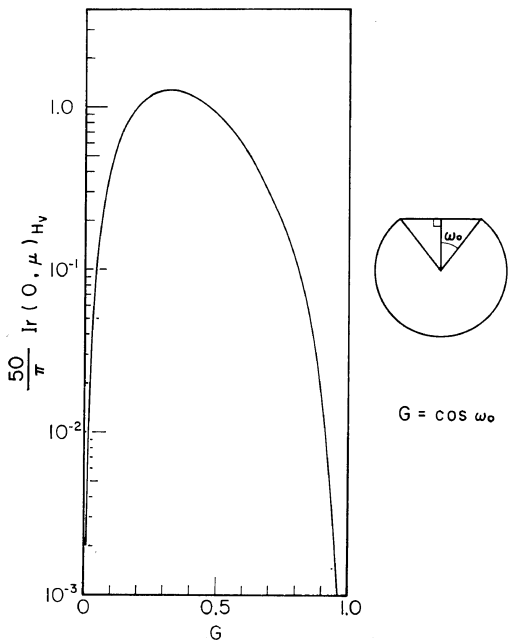

Figure 12. Change of relative intensity of scattered rays under the H_V polarization, $I_r(0, \mu)_{H_V}$, with the parameter G for the single-truncated circular disc texture.

The calculated results of $I_r(0, \mu)_{H_V}$ for the respective models from eq 20 to 24, are demonstrated in Figures 10 to 12. As seen in the Figures, the relative scattering intensity, $I_r(0, \mu)_{H_V}$ does not become zero, except for the circular or semicircular disc. Furthermore, as recognized from eq 20 for the sheaf-like (single) texture and from eq 24 for the single-truncated disc, both models give the semicircular disc as having $I_r(0, \mu)_{H_V}=0$ for $\omega_0=\pi/2$ and $G=0$, respectively.*

Figure 13 shows the contour plots of the H_V scattering intensity distributions for the respective models, demonstrating that the intensity distribution of the regular polygon becomes identical with that of the circular disc, when N is larger than 5, and that the intensity distribution changes considerably to have definite intensity at $\mu=0°$ and 90°, when the shape of the anisotropic body deviates from the circular disc.

* According to the calculation by Picot and Stein for the single-truncated spherulites,[5] the relative intensity, I_r (0, μ), does not become zero for $G=0$, suggesting a miscalculation (see Figure 5 in reference 5).

APPENDIX

In order to discuss the derivations of eq 3 and 4 through eq 2, in detail, suppose the following relation in general

$$f(\omega)=\int_{r=0}^{R(\omega)} \exp[ik(\boldsymbol{r}\cdot\boldsymbol{s})]r\,\mathrm{d}r \tag{A1}$$

where

$$R(\omega)=R_0 g(\omega) \tag{A2}$$

then the function $f(\omega)$ can be expanded in the following series

$$f(\omega)=R_0^2[\sum_{l=1} A_l\{g(\omega)\}^{2l}\{\cos(\omega+\beta)\}^{2(l-1)} - i\sum_{l=1} B_l\{g(\omega)\}^{2l+1}\{\cos(\omega+\beta)\}^{2l-1}] \tag{A3}$$

where

$$A_l=-\frac{(kR_0\sin\theta)^2}{2l(2l-3)}A_{l-1}$$

$$A_1=(1/2) \tag{A4}$$

$$B_l=-\frac{(kR_0\sin\theta)^2}{2(l-1)(2l+1)}B_{l-1}$$

$$B_1=kR_0\sin\theta/3 \tag{A5}$$

$$\beta=\theta_j-\mu\,. \tag{A6}$$

Therefore, the amplitudes of the scattered ray for the H_V and V_V polarization conditions may be given by

$$E(\theta_j)_{H_V}=\frac{\delta E_0 R_0^2}{2}[\sin 2\theta_j\sum_{l=1}\{E_1^l-iE_4^l\} -2\cos 2\theta_j\sum_{l=1}\{E_2^l-iE_5^l\}] \tag{A7}$$

$$E(\theta_j)_{V_V}=\frac{\delta E_0 R_0^2}{2}[\cos 2\theta_j\sum_{l=1}\{E_1^l-iE_4^l\} +2\sin 2\theta_j\sum_{l=1}\{E_2^l-iE_5^l\} +(1+2p)\sum_{l=1}\{E_3^l-iE_6^l\}] \tag{A8}$$

where

$$E_1^l=A_l\sum_{i=0}^{l-1}F_1^{li}(\cos\beta)^{2(l-i-1)}(\sin\beta)^{2i} \tag{A9}$$

$$F_1^{li}=\binom{2l-2}{2i}\int_0^{2\pi}\{g(\omega)\}^2 \times\cos 2\omega(\cos\omega)^{2(l-i-1)}(\sin\omega)^{2i}\,\mathrm{d}\omega \tag{A10}$$

$$E_2^{\,l}=-A_l\sum_{i=1}^{l-1}F_2^{\,li}(\cos\beta)^{2l-2i-1}(\sin\beta)^{2i-1} \quad \text{(A11)}$$

$$F_2^{\,li}=\binom{2l-2}{2i-1}\int_0^{2\pi}\{g(\omega)\}^2(\cos\omega)^{2(l-i)}(\sin\omega)^{2i}\,\mathrm{d}\omega \quad \text{(A12)}$$

$$E_3^{\,l}=A_l\sum_{i=0}^{l-1}F_3^{\,li}(\cos\beta)^{2(l-i-1)}(\sin\beta)^{2i} \quad \text{(A13)}$$

$$F_3^{\,li}=\binom{2l-2}{2i}\int_0^{2\pi}\{g(\omega)\}^2(\cos\omega)^{2(l-i-1)}(\sin\omega)^{2i}\,\mathrm{d}\omega \quad \text{(A14)}$$

$$E_4^{\,l}=B_l\sum_{i=0}^{l-1}F_4^{\,li}(\cos\beta)^{2l-2i-1}(\sin\beta)^{2i} \quad \text{(A15)}$$

$$F_4^{\,li}=\binom{2l-1}{2i}\int_0^{2\pi}\{g(\omega)\}^{2l+1}\times\cos 2\omega(\cos\omega)^{2l-2i-1}(\sin\omega)^{2i}\,\mathrm{d}\omega \quad \text{(A16)}$$

$$E_5^{\,l}=-B_l\sum_{i=0}^{l-1}F_5^{\,li}(\cos\beta)^{2(l-i-1)}(\sin\beta)^{2i+1} \quad \text{(A17)}$$

$$F_5^{\,li}=\binom{2l-1}{2i+1}\int_0^{2\pi}\{g(\omega)\}^{2l+1}\times(\cos\omega)^{2l-2i-1}(\sin\omega)^{2i+2}\,\mathrm{d}\omega \quad \text{(A18)}$$

$$E_6^{\,l}=B_l\sum_{i=0}^{l-1}F_6^{\,li}(\cos\beta)^{2l-2i-1}(\sin\beta)^{2i} \quad \text{(A19)}$$

$$F_6^{\,li}=\binom{2l-1}{2i}\int_0^{2\pi}\{g(\omega)\}^{2l+1}\times(\cos\omega)^{2l-2i-1}(\sin\omega)^{2i}\,\mathrm{d}\omega \quad \text{(A20)}$$

The scattering intensity, for example, for the H_V polarization can be given by

$$I(\theta,\mu)_{H_V}=\frac{K\delta^2E_0^{\,2}R_0^{\,4}}{4}\left[\int_0^{2\pi}\{\sin 2\theta_j\sum_{l=1}E_1^{\,l}-2\cos 2\theta_j\sum_{l=1}E_2^{\,l}\}^2+\int_0^{2\pi}\{\sin 2\theta_j\sum_{l=1}E_4^{\,l}-2\cos 2\theta_j\sum_{l=1}E_5^{\,l}\}^2\,\mathrm{d}\theta_j\right] \quad \text{(A21)}$$

$$=\frac{K\delta^2E_0^{\,2}R_0^{\,4}}{4}\left[\int_0^{2\pi}\{\sin 2(\beta+\mu)\sum_{l=1}E_1^{\,l}-2\cos 2(\beta+\mu)\sum_{l=1}E_2^{\,l}\}\,\mathrm{d}\beta+\int_0^{2\pi}\{\sin 2(\beta+\mu)\sum_{l=1}E_4^{\,l}-2\cos 2(\beta+\mu)\sum_{l=1}E_5^{\,l}\}\,\mathrm{d}\beta\right] \quad \text{(A22)}$$

$$=\frac{K\delta^2E_0^{\,2}R_0^{\,4}}{4}\left[\int_0^{2\pi}\left\{\frac{1-\cos 4(\beta+\mu)}{2}\sum_{l=1}E_5^{\,l}\sum_{m=1}E_1^{\,m}+2[1+\cos 4(\beta+\mu)]\sum_{l=1}E_2^{\,l}\sum_{m=1}E_2^{\,m}-2\sin 4(\beta+\mu)\sum_{l=1}E_1^{\,l}\sum_{m=1}E_2^{\,m}\right\}\mathrm{d}\beta+\int_0^{2\pi}\left\{\frac{1-\cos 4(\beta+\mu)}{2}\sum_{l=1}E_4^{\,l}\sum_{m=1}E_4^{\,m}+2[1+\cos 4(\beta+\mu)]\sum_{l=1}E_5^{\,l}\sum_{m=1}E_5^{\,m}-2\sin^4(\beta+\mu)\sum_{l=1}E_4^{\,l}\sum_{m=1}E_5^{\,m}\right\}\mathrm{d}\beta\right] \quad \text{(A23)}$$

$$=\frac{K\delta^2E_0^{\,2}R_0^{\,4}}{4}\left[\int_0^{2\pi}\left\{\frac{1-\cos 4\mu\cos 4\beta}{2}\sum_{l=1}A_l\sum_{m=1}A_m\times\sum_{i=0}^{l-1}F_1^{\,li}\sum_{j=0}^{m-1}F_1^{\,lj}(\cos\beta)^{2(l+m-i-j-2)}(\sin\beta)^{2(i+j)}+2(1+\cos 4\mu\cos 4\beta)\sum_{l=1}A_l\sum_{m=1}A_m\times\sum_{i=1}^{l-1}F_2^{\,li}\sum_{j=1}^{m-1}F_2^{\,mj}(\cos\beta)^{2(l+m-i-j-1)}(\sin\beta)^{2(i+j-1)}+2\cos 4\mu\sin 4\beta\sum_{l=1}A_l\sum_{m=1}A_m\times\sum_{i=0}^{l-1}F_1^{\,li}\sum_{j=1}^{m-1}F_2^{\,mj}(\cos\beta)^{2(l+m-i-j)-3}\times(\sin\beta)^{2(i+j)-1}\right\}\mathrm{d}\beta+\int_0^{2\pi}\left\{\frac{1-\cos 4\mu\cos 4\beta}{2}\sum_{l=1}B_l\sum_{m=1}B_m\times\sum_{i=0}^{l-1}F_4^{\,li}\sum_{j=0}^{m-1}F_4^{\,mj}(\cos\beta)^{2(l+m-i-j-1)}(\sin\beta)^{2(i+j)}+2(1+\cos 4\mu\cos 4\beta)\sum_{l=1}B_l\sum_{m=1}B_m\times\sum_{i=0}^{l-1}F_5^{\,li}\sum_{j=0}^{m-1}F_5^{\,mj}(\cos\beta)^{2(l+m-i-j-2)}(\sin\beta)^{2(i+j+1)}+2\cos 4\mu\sin 4\beta\sum_{l=1}B_l\sum_{m=1}B_m\times\sum_{i=0}^{l-1}F_4^{\,li}\sum_{j=0}^{m-1}F_5^{\,mj}(\cos\beta)^{2(l+m-i-j)-3}\times(\sin\beta)^{2(i+j)+1}\right\}\mathrm{d}\beta\right] \quad \text{(A24)}$$

When one separates the results of eq A24 into two parts by including or excluding $\cos 4\mu$, then eq 3 may be derived. Then scattering intensity distribution for the V_V polarization condition may be obtained, similarly to the above, from eq A8 to give eq 4.

Acknowledgements. A part of this work was supported by the grant from the Scientific

Research Funds (Kagaku Kenkyu-hi, 85181-1970) of the Ministry of Education, Japan, and the grants from the Toray Industries, Inc., Dai-Nippon Gosei Kagaku Co., Ltd., and Dai-Nippon Cellophane Mfg. Co., Ltd., Japan.

REFERENCES

1. R. S. Stein and M. B. Rhodes, *J. Appl. Phys.*, **31**, 1873 (1960).
2. S. B. Clough, J. J. van Aartsen, and R. S. Stein, *ibid.*, **36**, 8072 (1965).
3. M. Motegi, T. Oda, M. Moritani, and H. Kawai, *Polymer J.*, **1**, 209 (1970).
4. C. Picot, R. S. Stein, M. Motegi, and H. Kawai, *J. Polym. Sci., Part A-2*, **8**, 2115 (1970).
5. R. S. Stein and C. Picot, *ibid.*, **8**, 2127 (1970).
6. R. S. Stein and W. Chu, *ibid.*, **8**, 1137 (1970).
7. R. S. Stein and T. Hashimoto, *ibid.*, **9**, 517 (1971).
8. T. Hashimoto and R. S. Stein, *ibid.*, **9**, 1747 (1971).
9. M. Motegi, M. Moritani, and H. Kawai, *ibid.*, **8**, 499 (1970).
10. M. Moritani, N. Hayashi, A. Utsuo, and H. Kawai, *Polymer J.*, **2**, 74 (1971).
11. A. Tohdo, T. Hashimoto, and H. Kawai, submitted to *J. Polym. Sci., Part A-2*.